Growth of InGaN and double heterojunction structure with InGaN back barrier*

Shi Linyu(史林玉)†, Zhang Jincheng(张进城), Wang Hao(王昊), Xue Junshuai(薛军帅), Ou Xinxiu(欧新秀), Fu Xiaofan(付小凡), Chen Ke(陈珂), and Hao Yue(郝跃)

(Key Laboratory of Wide Band Gap Semiconductor Materials and Devices, Institutes of Microelectronics, Xidian University, Xi'an 710071, China)

Abstract: We study the growth of an InGaN and AlGaN/GaN/InGaN/GaN double heterojunction structure by metal organic chemical vapor deposition (MOCVD). It is found that the crystal quality of the InGaN back barrier layer significantly affects the electronic property of the AlGaN/GaN/InGaN/GaN double heterojunction. A high crystal quality InGaN layer is obtained by optimizing the growth pressure and temperature. Due to the InGaN layer polarization field opposite to that in the AlGaN layer, an additional potential barrier is formed between the GaN and the InGaN layer, which enhances carrier confinement of the 2DEG and reduces the buffer leakage current of devices. The double heterojunction high-electron-mobility transistors with an InGaN back barrier yield a drain induced barrier lowering of 1.5 mV/V and the off-sate source-drain leakage current is as low as 2.6 μA/mm at V_{DS} = 10 V.

Key words: InGaN back barrier; double hererojunction; carrier confinement
DOI: 10.1088/1674-4926/31/12/123001 **PACC:** 7280E; 7360L

1. Introduction

AlGaN/GaN heterostructures have attracted much attention for optoelectronic and electronic device applications[1, 2]. However, applications at the K band and above demand GaN-based amplifiers operating at higher frequencies, and the gate length (L_G) of the transistors has to be reduced below 0.4 μm. A major problem when scaling down these devices is the poor confinement of the 2DEG. Due to the electron spill over at high drain/gate voltages, peak currents are limited by the buffer leakage and large threshold-voltage shift, soft pinch-off, high subthreshold current. This effect contributes to the poor confinement of the 2DEG, so the double heterostructure of AlGaN/GaN/InGaN/GaN with an InGaN back barrier was put forward to improving the confinement of the 2DEG[3]. Although the band gap energy of InGaN is less than that of GaN, the larger polarization field which is opposite to the AlGaN layer can be formed between the InGaN and the GaN, which will raise the potential energy.

It is well known that high quality InGaN films are difficult to grow due to the high equilibrium vapor pressure of InN[4], as well as the indium separation behavior. Most of the growth of InGaN has been made by molecular beam epitaxy (MBE)[5, 6]. However, the growth of InGaN using metalorganic chemical vapor deposition (MOCVD) is very rare[7]. In this work, we adopt the pulse method for InGaN growth and study the performance of AlGaN/GaN/InGaN/GaN DH-HEMTs. Due to the InGaN back barrier layer, 2DEG confinement and buffer isolation were improved significantly.

2. Experimental procedures

The InGaN/GaN structures were grown on a sapphire substrate by a low-pressure MOCVD system. Figure 1 shows a schematic diagram of the samples and devices. Trimethylalumium (TMA), trimethylgallium (TEGa), trimethylindium (TMIn) and NH_3 were used as the sources of Al, Ga, In and N, respectively. Prior to epitaxial growth, sapphire substrates were annealed at 1050 ℃ for 10 min in order to remove surface contamination. A 100 nm thick high temperature AlN nucleation layer was deposited at 1020 ℃. Then, a 1.5 μm-thick unintentionally doped GaN layer was grown, followed by a 100 nm-thick InGaN layer. The pulse method was used for InGaN layer growth. In this method, NH_3 and TEGa flows were maintained continuously into the reaction chamber, while TMIn was injected into the reaction chamber alternately. Table 1 shows the temperature and pressure for the InGaN layer growth. For the conventional AlGaN/GaN heterostruture, the growth temperature for AlGaN barrier layers was 980 ℃. While for the three samples (samples D, E, G) of the AlGaN/GaN/InGaN/GaN double heterostructure, the GaN channel was deposited after the growth of the InGaN epilayer. The growth conditions of the InGaN layer are shown in Table 1. The growth temperature of the GaN was 670 ℃, which is used to reduce the indium out-diffusion.

The surface morphology of the heterostructures was investigated by an Agilent 5400 atomic force microscope (AFM). The indium composition of the samples was estimated by a 2θ–ω scan of (0002) plane diffraction of high resolution X-ray diffraction (HR XRD). The optical properties of the InGaN layers were examined by photoluminescence (PL) using a 325

Table 1. Growth conditions for the InGaN layer.

Parameter	Growth temperature (℃)	Growth pressure (Torr)
Sample A	670	40
Sample B	670	200
Sample C	650	200

* Project supported by the Major Program and Key Project of National Natural Science Foundation of China (Nos. 60890191, 60736033) and the National Key S&T Special Project (No. 2008ZX01002).
† Corresponding author. Email: sly_yolanda@163.com
Received 6 May 2010, revised manuscript received 19 July 2010

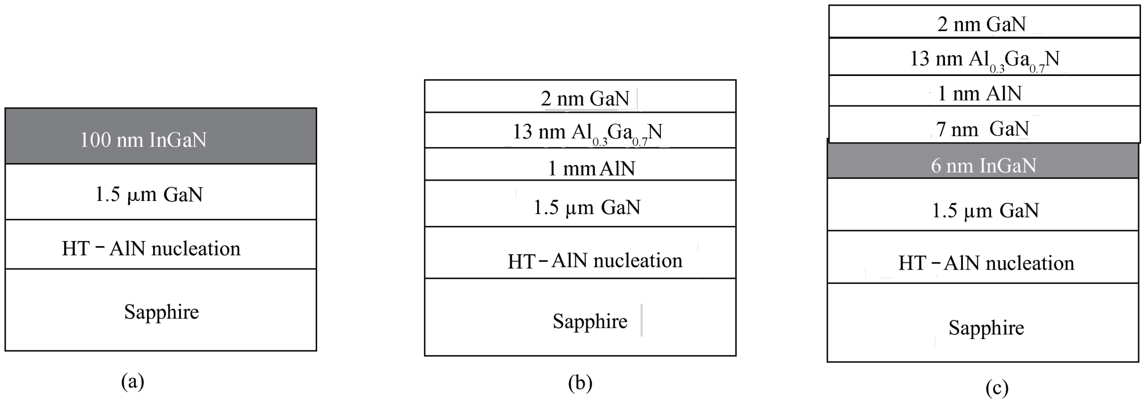

Fig. 1. Schematic cross section of the structures for (a) InGaN/GaN, (b) AlGaN/GaN, and (c) AlGaN/GaN/InGaN/GaN.

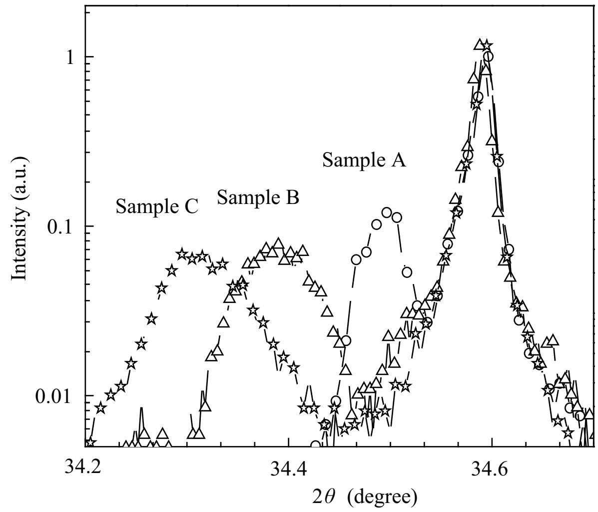

Fig. 2. XRD 2θ–ω scan curves of samples A, B and C.

nm He–Cd laser.

3. Results and discussion

In incorporation in InGaN layer is very sensitive to the growth temperature due to the extremely high equilibrium vapor pressure of InN[4]. The In incorporation is found to increase significantly as the growth temperature decreases[8]. Figure 2 shows the XRD $2\theta-\omega$ scan profiles of samples A, B and C. The peaks diffracted from GaN (0002) planes locate at about 34.6°. The reference value of the diffraction angle from InN (0002) is 31.0°[9]. Indium composition was estimated by XRD (0002) diffraction. When the total pressure increased, the diffraction peak position of the InGaN (0002) shifted from GaN to InN (0002), and the indium composition increased from ~3% to ~6% for samples A and B. This was attributed to the increasing total pressure which increased the absolute TMIn concentration in the reactor. As the growth temperature decreased, the peaks related to the InGaN shifted towards a lower angle, while the indium composition increased from ~6% to ~8% for samples B and C. These results confirmed that the indium content can be controlled by changing the growth pressure and temperature.

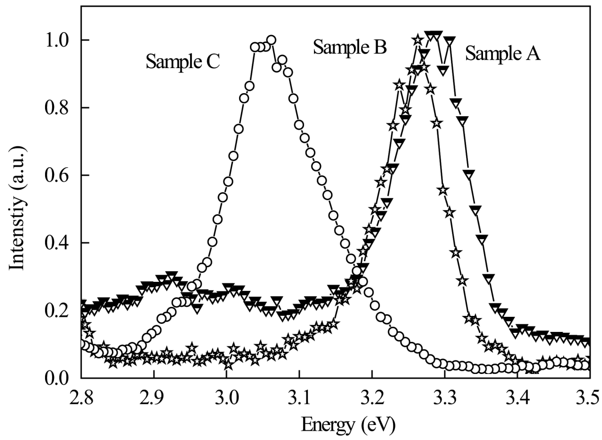

Fig. 3. PL spectra of samples A, B, and C.

Figure 3 shows the PL spectra of InGaN. The shift of the dominant emission peak moved towards a longer wavelength (from 3.3 to 3.05 eV) for samples A–C. Assuming that the indium composition in the InGaN layer can be determined only by the PL peak position, we calculated the indium contents in InGaN layer by

$$E(x) = E_{\rm GaN} - x(E_{\rm GaN} - E_{\rm InN}) - bx(1-x), \quad (1)$$

where $E_{\rm GaN}$, $E_{\rm InN}$, x, and b are the band gap energy of GaN, the band gap energy of InN, the indium composition and the bowing parameter, respectively. The indium content was calculated by using the parameters $E_{\rm GaN}$ (3.48 eV), $E_{\rm InN}$ (0.7 eV) and b (1.4 eV)[10]. Based on the PL peak position of InGaN, it was found that the indium composition in samples A–C was 3.5%, 5% and 8.5%, respectively. The full width half maximum (FWHM) values of the near band edge emission (NBE) for samples A–C were 100, 84.6 and 144 meV, respectively. From the FWHM values, we concluded that the InGaN film had better crystal quality with the 200 Torr growth press and 670 ℃ temperature.

Figure 4 shows the AFM images with a scan area of $2 \times 2\ \mu{\rm m}^2$ for each InGaN. From the AFM images, we found that the root mean square (RMS) roughness of the samples were 7, 1.04 and 8.02 nm for samples A, B, and C, respectively.

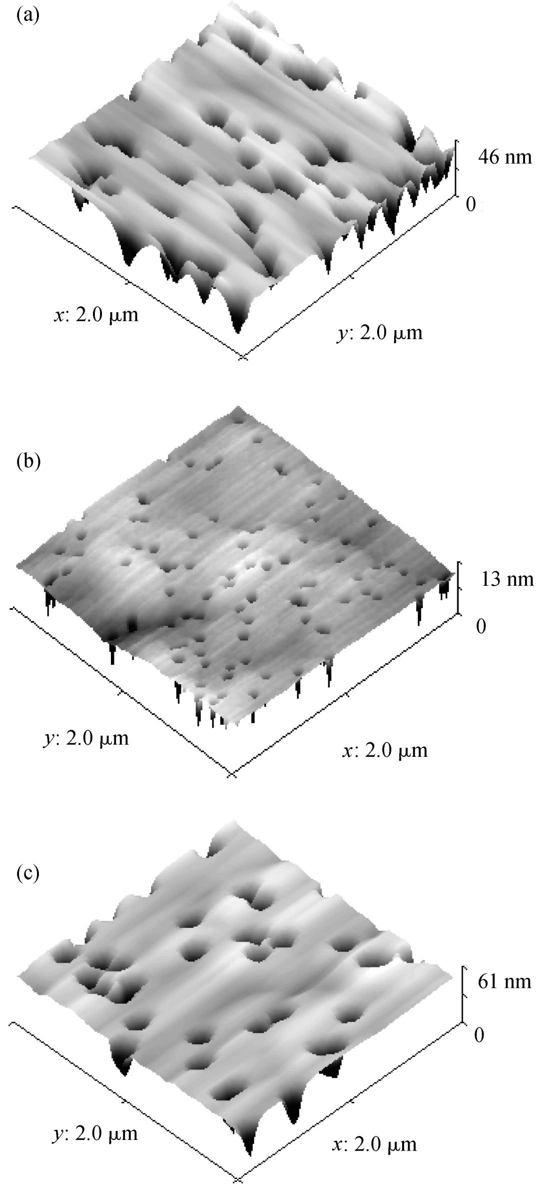

Fig. 4. 3D morphology of (a) sample A, (b) sample B, and (c) sample C.

Table 2. Electronic properties of the samples.

Parameter	Mobility ($cm^2/(V{\cdot}s)$)	2DEG density (10^{13} cm^{-2})
Sample D	1058	1.32
Sample E	1297	1.26
Sample G	940	1.2
SH	1288	1.55

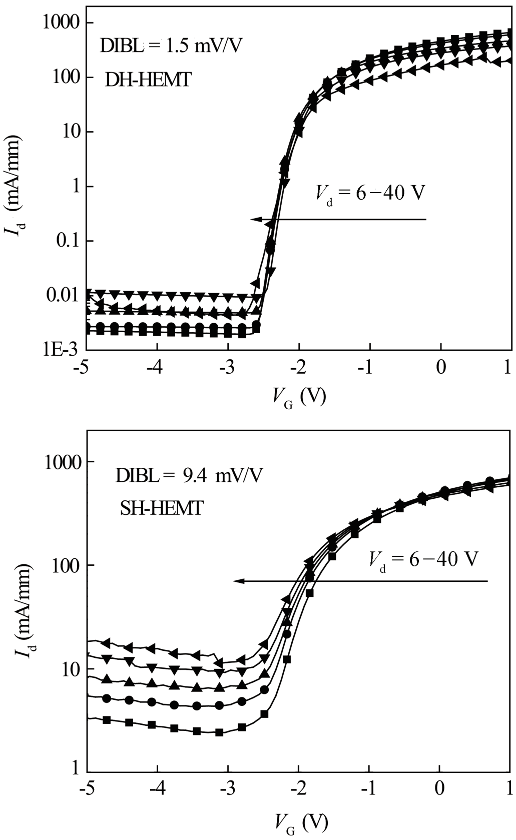

Fig. 5. Transfer characteristics for (a) AlGaN/GaN/InGaN/GaN DH-HEMT and (b) AlGaN/GaN SH-HEMT.

It can be seen clearly that the sample B had a flatter surface with a maximum height of 13 nm, while the maximum height of samples A and C were 46 and 61 nm, respectively. These holes, called V defects, were produced by local indium segregation around the dislocation cores, which emerged in the crystal growth[11]. The radius of the V pits in samples A, B, and C were 0.9, 0.38 and 1.4 Å, respectively. The results obtained by PL and AFM demonstrated that the crystal quality of sample B was the best and most suitable for the back barrier in the AlGaN/GaN/InGaN/GaN DH-HEMTs.

Table 2 shows that the AlGaN/GaN/InGaN/GaN double heterojunction exhibited the best electronic property at the growth temperature of 670 ℃ and pressure of 200 Torr for the InGaN back barrier layer. It is reported that the InGaN back barrier layer can enhance the confinement and thus improve the mobility of the 2DEG[12]. However, the double heterojunction electronic mobility obtained from our experiment was lower than that of the single one. This was attributed to the poor crystal quality of the InGaN layer.

Sample E and the AlGaN/GaN heterojunction were chosen for device fabrication. The mesa isolation was done first. Then, Ti/Al/Ni/Au was evaporated for source/drain ohmic contacts by rapid thermal annealing at 870 ℃ for 40 s. Finally, the Ni/Au Schottky gate was defined by optical lithography with an 80 nm nominal gate length. The DC performances of the HEMTs were measured with an HP 4156B semiconductor parameter analyzer.

From the measurement results, it can be seen that the advantage of the DH-HEMT over the SH-HEMT is lower buffer leakage current, which was 2.6 μA/mm measured at V_D = 10 V and much smaller than that of a conventional SH-HEMT device (6.8 mA/mm). Figure 5 shows the shift in threshold voltage (V_{TH}) with increasing drain voltage. The DH-HEMT device yielded a DIBL of 1.5 mV/V, while the SH-HEMT device exhibited a DIBL of 9.4 mV/V. When the drain voltage was varied by 6, 10, 20, 30 and 40 V, the resulting shift of V_{TH} was 0.05 V for the DH-HEMT and 0.32 V for the SH-HEMT. Due to the poor confinement, the electrons can spill over from channel to buffer under high drain voltage, which forms the buffer leakage current and leads the threshold voltage drift to be more negative. Breakdown in the GaN based HEMT and other field-effect devices is, in many cases, initiated by electron current underneath the depletion region of the transistor gate through the insulating buffer layer and is known as space-charge injection of electrons into the GaN buffer layer. The punchthrough of the electrons into the buffer causes a rapid increase in the sub-threshold drain leakage current and is often interpreted as the device breakdown voltage[13]. In case of large buffer leakage current, buffer breakdown will occur. The larger polarization field, which formed opposite to the AlGaN layer and between the InGaN and the GaN, raises the potential energy. The obstacle existing behind the quantum well hinders the electron spill over into the buffer and thus improves the buffer isolation.

4. Conclusions

In summary, we studied InGaN growth and AlGaN/GaN/InGaN/GaN DH-HEMT characteristics. For the realization of high quality AlGaN/GaN/InGaN/GaN DH-HEMT, different growth pressures and temperatures were adjusted to obtain high crystal quality InGaN back barrier layer. We got the best result under the growth temperature of 670 ℃ and pressure of 200 Torr for InGaN back barrier layer. Due to a high potential barrier between InGaN back barrier and GaN buffer layer, the buffer isolation is improved and the off-sate source-drain leakage current is as low as 2.6 μA/mm. The DH-HEMT exhibited a DIBL of 1.5 mV/V, which is smaller than that of SH-HEMT (9.4 mV/V). It suggests that high back potential barriers in DH-HEMT can prevent the electrons spilling into the buffer layer and confine the 2DEG in channel.

References

[1] Arulkumaran S, Egawa T, Ishikawa H, et al. High-temperature effects of AlGaN/GaN high-electron-mobility transistors on sapphire and semi-insulating SiC substrates. Appl Phys Lett, 2002, 80: 2186

[2] Xing H, Keller S, Wu Y F, et al. Gallium nitride based transistors. J Phys Condens Matter, 2001, 13: 7139

[3] Liu J, Zhou Y G, Zhu J, et al. DC and RF characteristics of AlGaN/GaN/InGaN/GaN double-heterojunction HEMTs. IEEE Electron Device Lett, 2006, 27(1): 10

[4] Matsuoka T, Tanaka H, Sasaki T, et al. Wide-gap semiconductor (In, Ga)N. Inst Phys Conf Ser, 1990, 106: 141

[5] Hori M, Kano K, Yamaguchi T, et al. Optical properties of $In_xGa_{1-x}N$ with entire alloy composition on InN buffer layer grown by RF-MBE. Phys Status Solidi B, 2002, 234: 750

[6] Wu J, Walukiewicz W, Yu K M, et al. Small band gap bowing in $In_{1-x}Ga_xN$ alloys. Appl Phys Lett, 2002, 80: 4741

[7] Chang C A, Shin C F, Chen N C, et al. In-rich $In_{1-x}Ga_xN$ films by metalorganic vapor phase epitaxy. Appl Phys Lett, 2004, 85: 6131

[8] Kim H J, Na H, Kwon S Y, et al. Growth of In-rich InGaN/GaN quantum dots by metalorganic chemical vapor deposition. J Cryst Growth, 2004, 269: 95

[9] Tansley T L, Foley C P. Optical band gap of indium nitride. J Appl Phys, 1986, 59: 3241

[10] Kim H J, Shin Y, Kwon S Y, et al. Compositional analysis of In-rich InGaN layers grown on GaN templates by metalorganic chemical vapor deposition. J Cryst Growth, 2008, 310: 3004

[11] Chen Y, Takeuchi T, Amino H, et al. Pit formation in GaInN quantum wells. Appl Phys Lett, 1998, 72:710

[12] Chen Y, Takeuchi T, Amino H, et al. Pit formation in GaInN quantum wells. Appl Phys Lett, 1998, 72: 710

[13] Tang J, Wang X, Chen T, et al. AlGaN/AlN/GaN/InGaN/GaN DH-HEMTs with improved mobility grown by MOCVD. 9th International Conference on Solid-State and Integrated-Circuit Technology, ICSICT, 2008: 1114

[14] Bahat-Treidel E, Hilt O, Brunner F, et al. Punch through-voltage enhancement of AlGaN/GaN HEMTs using AlGaN double-heterojunction confinement. IEEE Trans Electron Device, 2008, 55: 12